PHYSICAL REVIEW D, VOLUME 61, 071101(R)

Update of the search for the neutrinoless decay $\tau \to \mu\gamma$

S. Ahmed, M. S. Alam, S. B. Athar, L. Jian, L. Ling, A. H. Mahmood,* M. Saleem, S. Timm, and F. Wappler
State University of New York at Albany, Albany, New York 12222

A. Anastassov, J. E. Duboscq, K. K. Gan, C. Gwon, T. Hart, K. Honscheid, H. Kagan, R. Kass, J. Lorenc, T. K. Pedlar, H. Schwarthoff, E. von Toerne, and M. M. Zoeller
Ohio State University, Columbus, Ohio 43210

S. J. Richichi, H. Severini, P. Skubic, and A. Undrus
University of Oklahoma, Norman, Oklahoma 73019

S. Chen, J. Fast, J. W. Hinson, J. Lee, N. Menon, D. H. Miller, E. I. Shibata, I. P. J. Shipsey, and V. Pavlunin
Purdue University, West Lafayette, Indiana 47907

D. Cronin-Hennessy, Y. Kwon,† A. L. Lyon, and E. H. Thorndike
University of Rochester, Rochester, New York 14627

C. P. Jessop, H. Marsiske, M. L. Perl, V. Savinov, D. Ugolini, and X. Zhou
Stanford Linear Accelerator Center, Stanford University, Stanford, California 94309

T. E. Coan, V. Fadeyev, I. Korolkov, Y. Maravin, I. Narsky, R. Stroynowski, J. Ye, and T. Wlodek
Southern Methodist University, Dallas, Texas 75275

M. Artuso, R. Ayad, E. Dambasuren, S. Kopp, G. Majumder, G. C. Moneti, R. Mountain, S. Schuh, T. Skwarnicki, S. Stone, G. Viehhauser, J. C. Wang, A. Wolf, and J. Wu
Syracuse University, Syracuse, New York 13244

S. E. Csorna, K. W. McLean, Sz. Márka, and Z. Xu
Vanderbilt University, Nashville, Tennessee 37235

R. Godang, K. Kinoshita,‡ I. C. Lai, and S. Schrenk
Virginia Polytechnic Institute and State University, Blacksburg, Virginia 24061

G. Bonvicini, D. Cinabro, L. P. Perera, and G. J. Zhou
Wayne State University, Detroit, Michigan 48202

G. Eigen, E. Lipeles, M. Schmidtler, A. Shapiro, W. M. Sun, A. J. Weinstein, and F. Würthwein§
California Institute of Technology, Pasadena, California 91125

D. E. Jaffe, G. Masek, H. P. Paar, E. M. Potter, S. Prell, and V. Sharma
University of California, San Diego, La Jolla, California 92093

D. M. Asner, A. Eppich, J. Gronberg, T. S. Hill, D. J. Lange, R. J. Morrison, and H. N. Nelson
University of California, Santa Barbara, California 93106

R. A. Briere
Carnegie Mellon University, Pittsburgh, Pennsylvania 15213

B. H. Behrens, W. T. Ford, A. Gritsan, J. Roy, and J. G. Smith
University of Colorado, Boulder, Colorado 80309-0390

J. P. Alexander, R. Baker, C. Bebek, B. E. Berger, K. Berkelman, F. Blanc, V. Boisvert, D. G. Cassel, M. Dickson, P. S. Drell, K. M. Ecklund, R. Ehrlich, A. D. Foland, P. Gaidarev, R. S. Galik, L. Gibbons, B. Gittelman, S. W. Gray, D. L. Hartill, B. K. Heltsley, P. I. Hopman, C. D. Jones, D. L. Kreinick, M. Lohner, T. O. Meyer, N. B. Mistry, C. R. Ng, E. Nordberg, J. R. Patterson, D. Peterson, D. Riley, J. G. Thayer, P. G. Thies, B. Valant-Spaight, and A. Warburton
Cornell University, Ithaca, New York 14853

P. Avery, C. Prescott, A. I. Rubiera, J. Yelton, and J. Zheng
University of Florida, Gainesville, Florida 32611

0556-2821/2000/61(7)/071101(6)/$15.00

G. Brandenburg, A. Ershov, Y. S. Gao, D. Y.-J. Kim, and R. Wilson
Harvard University, Cambridge, Massachusetts 02138

T. E. Browder, Y. Li, J. L. Rodriguez, and H. Yamamoto
University of Hawaii at Manoa, Honolulu, Hawaii 96822

T. Bergfeld, B. I. Eisenstein, J. Ernst, G. E. Gladding, G. D. Gollin, R. M. Hans, E. Johnson, I. Karliner, M. A. Marsh, M. Palmer, C. Plager, C. Sedlack, M. Selen, J. J. Thaler, and J. Williams
University of Illinois, Urbana-Champaign, Illinois 61801

K. W. Edwards
Carleton University, Ottawa, Ontario, Canada K1S 5B6 and the Institute of Particle Physics, Canada

R. Janicek and P. M. Patel
McGill University, Montréal, Québec, Canada H3A 2T8 and the Institute of Particle Physics, Canada

A. J. Sadoff
Ithaca College, Ithaca, New York 14850

R. Ammar, P. Baringer, A. Bean, D. Besson, R. Davis, I. Kravchenko, N. Kwak, and X. Zhao
University of Kansas, Lawrence, Kansas 66045

S. Anderson, V. V. Frolov, Y. Kubota, S. J. Lee, R. Mahapatra, J. J. O'Neill, R. Poling, T. Riehle, A. Smith, and J. Urheim
University of Minnesota, Minneapolis, Minnesota 55455

(CLEO Collaboration)

(Received 25 October 1999; revised manuscript received 5 January 2000; published 8 March 2000)

We present an update of the search for the lepton family number violating decay $\tau\to\mu\gamma$ using 12.6 million $\tau^+\tau^-$ pairs collected with the CLEO detector. No evidence of a signal has been found and the corresponding upper limit is $\mathcal{B}(\tau\to\mu\gamma)<1.1\times10^{-6}$ at 90% C.L., significantly smaller than previous experimental limits.

PACS number(s): 13.35.Dx, 11.30.Fs, 14.60.Fg

Nonconservation of the lepton flavor is expected in many extensions of the standard model and searches for lepton flavor violating decays provide strong constraints on possible new physics processes. Although there are many possible τ decay channels which do not conserve the lepton flavor number, the decay $\tau\to\mu\gamma$ is favored by most theoretical extensions of the standard model [1]. The most optimistic predictions for rates of such decays are based on the supersymmetric models [2–4], on the left-right supersymmetric models [5] and on the supersymmetric string unified models [6]. Recent calculations [4,6] predict values for the branching fraction of the decay $\tau\to\mu\gamma$ at the order of a few times 10^{-6} for some ranges of model parameters. In general, the expectations for all other lepton number or lepton flavor violating decays of the τ are at least an order of magnitude lower. Experimental searches for the $\tau\to\mu\gamma$ decay are limited by the number of observed τ decays. The lowest upper limit [7] of $\mathcal{B}(\tau\to\mu\gamma)<3.0\times10^{-6}$ at 90% C.L. has been published by the CLEO Collaboration using 4.24 million $\tau^+\tau^-$ pairs. The results presented here supersede the results of the previous CLEO analysis [7].

In this analysis we use a data sample from the reaction $e^+e^-\to\tau^+\tau^-$ collected at the Cornell Electron Storage Ring (CESR) at or near the energy of the $\Upsilon(4S)$. The data correspond to a total integrated luminosity of 13.8 fb^{-1} and contain 12.6 million $\tau^+\tau^-$ pairs. The CLEO detector components employed here are described in Refs. [8,9]. The event selection follows the procedure used in the previous search [7]. We select events with a 1-vs-1 topology, where the signal candidate τ decays into $\mu\gamma$ and the tag side includes all standard τ decays into one charged particle, any number of photons and at least one neutrino.

We select $\tau^+\tau^-$ pair events with exactly two good charged tracks, with total charge equal to zero, and with the angle between the charged tracks greater than 90°. Because radiative μ-pair production produces high background rates, we allow only one identified muon per event. In addition, each candidate event must have exactly one photon separated by more than 20° from the closest charged track projection

*Permanent address: University of Texas - Pan American, Edinburg TX 78539.

†Permanent address: Yonsei University, Seoul 120-749, Korea.

‡Permanent address: University of Cincinnati, Cincinnati OH 45221.

§Permanent address: Massachusetts Institute of Technology, Cambridge, MA 02139.

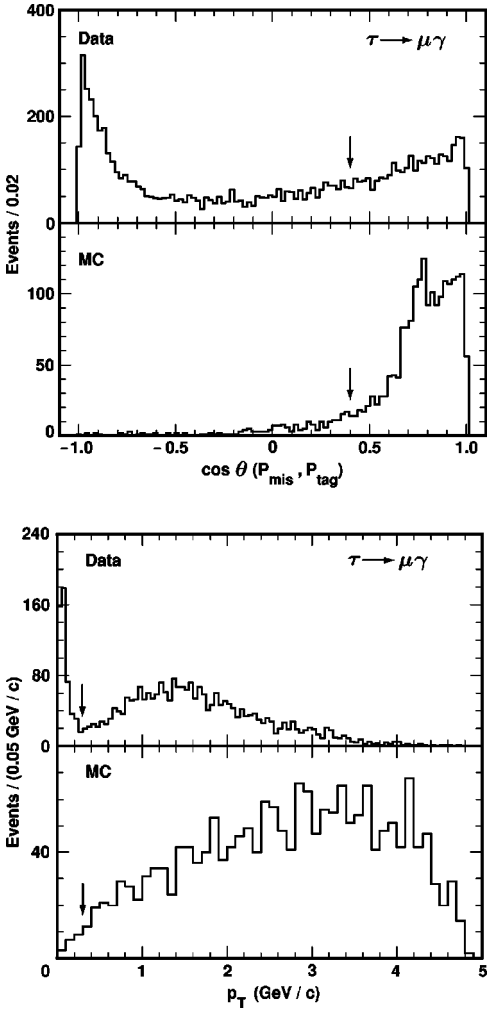

FIG. 1. Cosine of the angle between the total missing momentum of the event and the momentum of the tagging particle (top) and the total transverse momentum of the event (bottom) for data and a signal Monte Carlo sample. The imposed selection requirements are shown with arrows.

onto the calorimeter in the muon hemisphere. This photon must lie in the calorimeter barrel (i.e., $|\cos\theta_\gamma|<0.71$, where θ_γ is an angle between the photon and beam direction), have a photon-like lateral profile and have energy deposition in the calorimeter greater than 300 MeV. This minimum energy cut is dictated by the kinematics of a 2-body τ decay. The angle between the direction of the photon and the momentum of the muon track must satisfy $0.4<\cos\theta_{\mu\gamma}<0.8$, where the upper limit is again dictated by kinematics, and the lower limit is obtained by optimizing the signal-to-background ratio.

The main sources of background in the selected samples are due to μ-pair production, radiative $\tau\to\mu\gamma\nu\nu$ decays, and two-photon processes. To minimize these backgrounds, we require that the cosine of the angle between the total missing momentum of the event and the momentum of the tagging particle be greater than 0.4. The missing momentum is calculated as the negative of the sum of momenta of the two charged tracks and all neutral showers detected in the calorimeter with energies above 30 MeV. Because there

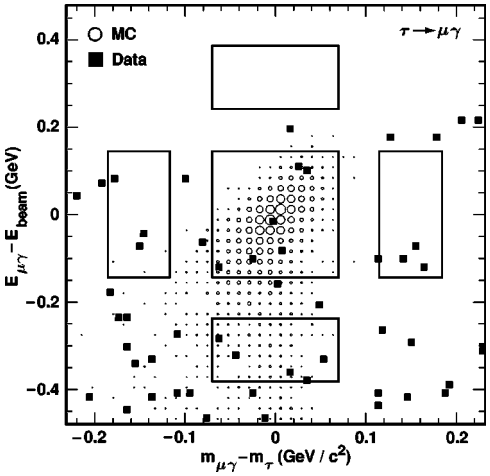

FIG. 2. $(E_{\mu\gamma}-E_{beam})$ vs $(m_{\mu\gamma}-m_\tau)$ distribution. The data are shown with solid squares and the signal Monte Carlo distribution is shown with open circles. The central box ($\pm 3\sigma$) represents the signal region and the four other boxes represent the sidebands. The region shown in this plot is within $\pm 10\sigma$ from the nominal τ mass and beam energy.

must be at least one undetected neutrino on the tag side, the missing momentum in an event having $\tau\to\mu\gamma$ is expected to fall into the tagging track hemisphere, while for all radiative processes the missing momentum should be uncorrelated with the charged track on the tag side. The neutrino emission on the tag side should also result in a large total transverse momentum with respect to the beam direction. Thus, to suppress background produced by copious two-photon and radiative QED processes, we require that the total transverse momentum of the event be greater than 300 MeV/c. The distribution of the cosine of the angle between the total missing momentum of the event and the momentum of the tagging particle as well as the distribution of the total transverse momentum for data and a signal Monte Carlo sample are

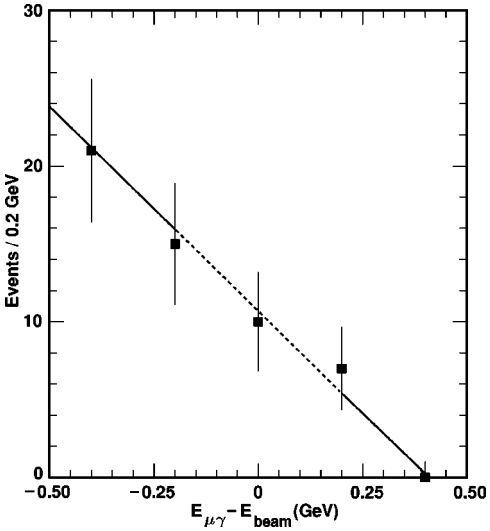

FIG. 3. $(E_{\mu\gamma}-E_{beam})$ distribution observed in the data with a linear fit superimposed. The signal region is excluded from the fit. The χ^2 of this fit is 0.4 for 2 degrees of freedom.

TABLE I. Selection efficiencies, numbers of events, and upper limits calculated with and without systematic errors.

	Method of Ref. [7]	Unbinned EML fit
MC efficiency, ϵ	$(12.7\pm0.2)\%$	$(15.2\pm0.2)\%$
Number of signal events	$n_0=6$	$s=1.8$
Expected background rate, b	5.5 ± 0.5	-
Statistical significance of the signal	-	1.0σ
Upper limit at 90% C.L., s_0	5.8	3.8
Upper limit for $\mathcal{B}(\tau\to\mu\gamma)$ at 90% C.L.	1.8×10^{-6}	1.0×10^{-6}
Upper limit at 90% C.L. with systematic error included	1.8×10^{-6}	1.1×10^{-6}

shown in Fig. 1. The selection efficiency of all requirements above is estimated from Monte Carlo simulation as $(16.2\pm0.2)\%$.

Final signal selection criteria are based on kinematic constraints since a neutrinoless τ decay should have a total energy and an effective mass of the $\mu\gamma$ consistent with the beam energy and τ mass, respectively. To determine these final criteria, we employ two different techniques. First, we follow the method outlined in CLEO's previous search [7] for the decay $\tau\to\mu\gamma$. Then we perform a more sensitive analysis based on an unbinned extended maximum likelihood (EML) fit to the data.

Following the method described in detail in Ref. [7], we parametrize the signal Monte Carlo mass and energy distributions separately as tailed Gaussian densities. Initial and final state radiation produces an asymmetric tail in energy, and both mass and energy distributions are slightly distorted by an asymmetric response of the calorimeter. The energy density is given by

$$f(E)=\begin{cases}\{l/[\,\eta(-\tilde{E}+l/\eta-\eta)]\}^l\exp(-\eta^2/2), & \tilde{E}<-\eta,\\ \exp(-\tilde{E}^2/2), & \tilde{E}>-\eta,\end{cases} \tag{1}$$

where $\tilde{E}=(E-E_{beam})/\sigma_E$ and σ_E, η, and l are the fit parameters. A similar formula is used for the invariant mass of the $\mu\gamma$ system, $\tilde{m}=(m-m_\tau)/\sigma_m$. The τ mass, m_τ, is taken to be 1.777 GeV/c^2 [10], and the beam energy E_{beam} varies from 5.26 to 5.29 GeV. The obtained Gaussian resolutions are $\sigma_m=23.2\pm0.4$ MeV/c^2 and $\sigma_E=47.9\pm1.2$ MeV. The signal region is then defined to be within ±3 standard deviations of the fitted Gaussian component of the distribution. There are 6 events observed in the signal region shown as the central box in Fig. 2. To estimate the amount of background expected in the signal region, we extrapolate the data from the sideband. We assume that the background distributions are linear in the vicinity of m_τ and E_{beam} and define the sideband regions to be between 5 and 8 standard deviations as shown in Fig. 2. To estimate the background uncertainty associated with this technique, we vary the sideband definition. The total expected background in the signal region is estimated as 5.5 ± 0.5 events.

The upper limit on the $\tau\to\mu\gamma$ branching fraction is estimated following the Bayesian prescription [11,12]

$$\frac{e^{-(s_0+b)}\sum_{n=0}^{n_0}(s_0+b)^n/n!}{e^{-b}\sum_{n=0}^{n_0}b^n/n!}=0.1, \tag{2}$$

where s_0 is an upper limit on the number of events in the signal region at 90% C.L., b is the expected background rate, and n_0 is the number of observed events. The upper limit on the branching fraction is then

$$\mathcal{B}(\tau\to\mu\gamma)<\frac{s_0}{2\epsilon N_{\tau\tau}}\ \text{at 90\% C.L.}, \tag{3}$$

where ϵ is the event selection efficiency and $N_{\tau\tau}$ is the total number of τ-pairs produced. Applying this technique, we obtain an upper limit on the branching fraction $\mathcal{B}(\tau\to\mu\gamma)$ of 1.8×10^{-6} at 90% C.L.

The systematic uncertainty in detector sensitivity $2\epsilon N_{\tau\tau}$ is conservatively estimated as 10%. This uncertainty is obtained by adding in quadrature uncertainties in track reconstruction efficiency (3%), photon reconstruction efficiency (5%), cut selection (5%), luminosity and cross-section (1.4%), lepton identification (4%), Monte Carlo statistics (1.5%) and trigger efficiency (5%). The upper limit for the branching fraction is also affected by the uncertainty in the background estimate of 0.5 events. To incorporate systematic uncertainty into the upper limit, we assume that the errors related to $2\epsilon N_{\tau\tau}$ and to the background estimate have Gaussian distributions and apply a technique described in Refs. [7,13]. This technique reweights the probability (2) by a Gaussian probability density of the detector sensitivity $2\epsilon N_{\tau\tau}$ and a Gaussian probability density of the number of background events b. The incorporation of these systematic uncertainties increases the upper limit by 1.9% of itself.

A more sensitive upper limit is obtained by performing an unbinned EML fit which takes into account the details of the distributions and correlations between the mass and energy of signal event candidates. The likelihood function is defined as

$$\mathcal{L}(s,b)=\frac{e^{-(s+b)}}{N!}\prod_{i=1}^{N}(sS_i+bB_i), \tag{4}$$

where N is the number of events in the signal region and its vicinity, s and b are the numbers of signal and background events, respectively, and S_i and B_i are the signal and background densities, respectively. The signal distribution is described by a two-dimensional Gaussian and a non-Gaussian tail in energy produced by initial and final state radiation, and an asymmetric response of the calorimeter. This tail covers the region below the beam energy and is modeled by a gamma function:

$$S_i(m,E)=\frac{A_G}{2\pi\sigma_m\sigma_E\sqrt{1-\rho^2}}\exp\left[-\frac{1}{2(1-\rho^2)}(\tilde{m}^2-2\rho\tilde{m}\tilde{E}+\tilde{E}^2)\right]+A_T\zeta(m,E);$$

$$\zeta(m,E)=\begin{cases}\dfrac{1}{\sqrt{2\pi}\sigma_m}\exp(-\tilde{m}^2/2)\dfrac{1}{\sigma_E\Gamma(\alpha)\beta^\alpha}(-\tilde{E})^{\alpha-1}\exp(\tilde{E}/\beta) & \text{if } \tilde{E}<0;\\ 0 & \text{otherwise,}\end{cases} \tag{5}$$

where A_G and A_T are the relative contributions of the Gaussian component and the non-Gaussian tail with the sum of A_G+A_T constrained to unity, σ_m and σ_E are mass and energy resolutions, respectively, ρ is the correlation coefficient, and α and β define the shape of the non-Gaussian tail $\zeta(m,E)$. To obtain the parameters of the signal density S_i, we fit the signal Monte Carlo distribution. The extracted value of the correlation coefficient is $\rho=0.625\pm0.012$, the relative areas A_G and A_T are 0.81 ± 0.02 and 0.19 ± 0.02, respectively, and the resolutions σ_m and σ_E are close to those obtained in the one-dimensional fits (1). The background is parametrized by a function linear in energy with the coefficients a_0 and a_1 obtained from a fit to the data:

$$B_i(m,E)=\frac{1}{m_2-m_1}\frac{1}{(a_0-a_1E_{beam})(E_2-E_1)+0.5a_1(E_2^2-E_1^2)}[a_0+a_1(E-E_{beam})], \tag{6}$$

where (m_1,m_2) and (E_1,E_2) are the limits defining the fit region. The projection of this fit onto the energy axis is shown in Fig. 3. The region within 4 standard deviations near the beam energy E_{beam} is excluded from the fit to avoid bias caused by the possible presence of real signal events in this region. Mean values and uncertainties of the background shape parameters a_0 and a_1 are estimated by varying the number of bins in the fit region with unit step from 5 to 12.

The EML fit to the data gives the number of candidates for the decay $\tau\to\mu\gamma$ as 1.8 events with an estimated statistical significance of the signal 1.0 standard deviations. The fit region, shown in Fig. 2, is defined to be within 10 standard deviations near the τ mass and beam energy. The total number of events in the fit region is 53. The confidence level of this fit estimated with toy Monte Carlo is 54%.

To estimate the upper limit, we use a method [14] developed for unbinned EML fits.[1] The expected number of background events is fixed at the value extracted from the EML fit to the data. For every assumed expected number of signal events s, we generate 10,000 Monte Carlo samples. For every sample, we generate numbers of signal and background events using Poisson distributions and then we generate positions of these events on the energy-vs-mass plane using the densities from Eqs. (5) and (6). For each sample we then perform an unbinned EML fit to extract the number of signal events, following the same procedure as for the data. The confidence level corresponding to this value of s is defined as a fraction of samples where the extracted number of events exceeds that observed in the data, i.e., 1.8. We repeat this procedure until we find a value of $s=s_0$ that gives a 90% C.L. This value has to be divided by the selection efficiency and the number of produced τ-pairs in accordance with Eq. (3). The obtained upper limit on the branching fraction $\mathcal{B}(\tau\to\mu\gamma)$ is 1.0×10^{-6} at 90% C.L.

To incorporate systematic uncertainty into this result, we smear the background shape parameters a_0 and a_1 within the estimated errors assuming Gaussian distributions and taking into account the correlation between these two parameters. We then repeat the procedure described in the previous paragraph integrating the likelihood function over the parameter space of a_0 and a_1. We do not observe a significant signal contribution, and the parameters of the signal density are known with high accuracy; thus, the effect of uncertainties in these parameters is negligible. In addition to smearing the background shape, we integrate the quantity $1/(2\epsilon N_{\tau\tau})$ assuming a Gaussian distribution for the detector sensitivity $2\epsilon N_{\tau\tau}$ with a relative standard deviation equal to the estimated systematic uncertainty of 10%. The incorporation of these systematic uncertainties increases the upper limit by 13% of itself. This uncertainty is dominated by the errors in the background shape parameters.

[1]This method assumes a confidence interval to be of the form $(0,s_0)$ and thus gives a different upper limit than that obtained by the method of Ref. [15]. The prescription [15] has been developed for problems with integer numbers of observed signal candidate events and, in its present shape, is inapplicable to EML fits.

The signal Monte Carlo sample used in this analysis was generated with a phase-space matrix element. However, various models [4,6] predict different structures of the current mediating the decay $\tau \to \mu\gamma$. This may result in different angular distributions of this decay. The two limiting angular distributions correspond to pure $V+A$ and $V-A$ exchanges. To account for the uncertainty due to the choice of the matrix element, we generated Monte Carlo samples with pure $V-A$ and pure $V+A$ structures of the current. Within statistical uncertainties, we find that the choice of the matrix element does not affect the energy and invariant mass resolutions or the correlation between these two variables. The selection efficiencies for the $V-A$ and $V+A$ currents are also equal to that for the phase-space model within statistical errors. Thus, the upper limit is insensitive to the choice of the matrix element.

The selection efficiencies, numbers of events, and upper limits calculated with and without inclusion of systematic errors for both techniques are given in Table I. This result is limited by the total integrated luminosity and represents a significant improvement over the previous analysis [7]. The obtained upper limit of 1.1×10^{-6} restricts the parameter space of models [4,6].

We gratefully acknowledge the effort of the CESR staff in providing us with excellent luminosity and running conditions. I.P.J. Shipsey thanks the NYI program of the NSF, M. Selen thanks the PFF program of the NSF, M. Selen and H. Yamamoto thank the OJI program of DOE, M. Selen and V. Sharma thank the A.P. Sloan Foundation, M. Selen and V. Sharma thank the Research Corporation, F. Blanc thanks the Swiss National Science Foundation, and H. Schwarthoff and E. von Toerne thank the Alexander von Humboldt Stiftung for support. This work was supported by the National Science Foundation, the U.S. Department of Energy, and the Natural Sciences and Engineering Research Council of Canada.

[1] R. Stroynowski, Nucl. Phys. B (Proc. Suppl.) **76**, 185 (1999).
[2] R. Barbieri and L.J. Hall, Phys. Lett. B **338**, 212 (1994).
[3] J. Hisano *et al.*, Phys. Lett. B **357**, 579 (1995).
[4] J. Hisano and D. Nomura, Phys. Rev. D **59**, 116005 (1999).
[5] K.S. Babu, B. Dutta, and R.N. Mohapatra, Phys. Lett. B **458**, 93 (1999).
[6] S.F. King and M. Oliveira, Phys. Rev. D **60**, 035003 (1999).
[7] CLEO Collaboration, K.W. Edwards *et al.*, Phys. Rev. D **55**, R3919 (1997).
[8] Y. Kubota *et al.*, Nucl. Instrum. Methods Phys. Res. A **320**, 66 (1992).
[9] T.S. Hill, Nucl. Instrum. Methods Phys. Res. A **418**, 32 (1998).
[10] Particle Data Group, C. Caso *et al.*, Eur. Phys. J. C **3**, 1 (1998).
[11] O. Helene, Nucl. Instrum. Methods Phys. Res. **212**, 319 (1983).
[12] Particle Data Group, R.M. Barnett *et al.*, Phys. Rev. D **54**, 1 (1996), p. 159.
[13] R. Cousins and V. Highland, Nucl. Instrum. Methods Phys. Res. A **320**, 331 (1992).
[14] I. Narsky, ''Estimation of upper limits using a Poisson statistic,'' hep-ex/9904025 (1999).
[15] G.J. Feldman and R.D. Cousins, Phys. Rev. D **57**, 3873 (1998).